Evidence for a narrow |S| = 1 baryon state at a mass of 1528 MeV in quasi-real photoproduction

A. Airapetian,[31] N. Akopov,[31] Z. Akopov,[31] M. Amarian,[8,31] V.V. Ammosov,[23] A. Andrus,[16] E.C. Aschenauer,[8]
W. Augustyniak,[30] R. Avakian,[31] A. Avetissian,[31] E. Avetissian,[12] P. Bailey,[16] D. Balin,[22] V. Baturin,[22]
M. Beckmann,[7] S. Belostotski,[22] S. Bernreuther,[10] N. Bianchi,[12] H.P. Blok,[21,29] H. Böttcher,[8] A. Borissov,[18]
A. Borysenko,[12] M. Bouwhuis,[16] J. Brack,[6] A. Brüll,[17] V. Bryzgalov,[23] G.P. Capitani,[12] T. Chen,[4] X. Chen,[4]
H.C. Chiang,[16] G. Ciullo,[11] M. Contalbrigo,[11] P.F. Dalpiaz,[11] W. Deconinck,[18] R. De Leo,[3] L. De Nardo,[1]
E. De Sanctis,[12] E. Devitsin,[19] P. Di Nezza,[12] M. Düren,[14] M. Ehrenfried,[10] A. Elalaoui-Moulay,[2] G. Elbakian,[31]
F. Ellinghaus,[8] U. Elschenbroich,[13] J. Ely,[6] R. Fabbri,[11] A. Fantoni,[12] A. Fechtchenko,[9] L. Felawka,[27] B. Fox,[6]
S. Frullani,[25] G. Gapienko,[23] V. Gapienko,[23] F. Garibaldi,[25] K. Garrow,[1,26] E. Garutti,[21] D. Gaskell,[6]
G. Gavrilov,[7,27] V. Gharibyan,[31] G. Graw,[20] O. Grebeniouk,[22] L.G. Greeniaus,[1,27] I.M. Gregor,[8] K. Hafidi,[2]
M. Hartig,[27] D. Hasch,[12] D. Heesbeen,[21] M. Henoch,[10] R. Hertenberger,[20] W.H.A. Hesselink,[21,29]
A. Hillenbrand,[10] M. Hoek,[14] Y. Holler,[7] B. Hommez,[13] G. Iarygin,[9] A. Ivanilov,[23] A. Izotov,[22] H.E. Jackson,[2]
A. Jgoun,[22] R. Kaiser,[15] E. Kinney,[6] A. Kisselev,[22] M. Kopytin,[8] V. Korotkov,[23] V. Kozlov,[19] B. Krauss,[10]
V.G. Krivokhijine,[9] L. Lagamba,[3] L. Lapikás,[21] A. Laziev,[21,29] P. Lenisa,[11] P. Liebing,[8] L.A. Linden-Levy,[16]
K. Lipka,[8] W. Lorenzon,[18] H. Lu,[5] J. Lu,[27] S. Lu,[14] X. Lu,[4] B.-Q. Ma,[4] B. Maiheu,[13] N.C.R. Makins,[16] Y. Mao,[4]
B. Marianski,[30] H. Marukyan,[31] F. Masoli,[11] V. Mexner,[21] N. Meyners,[7] O. Mikloukho,[22] C.A. Miller,[1,27]
Y. Miyachi,[28] V. Muccifora,[12] A. Nagaitsev,[9] E. Nappi,[3] Y. Naryshkin,[22] A. Nass,[10] M. Negodaev,[8] W.-D. Nowak,[8]
K. Oganessyan,[7,12] H. Ohsuga,[28] N. Pickert,[10] S. Potashov,[19] D.H. Potterveld,[2] M. Raithel,[10] D. Reggiani,[11]
P.E. Reimer,[2] A. Reischl,[21] A.R. Reolon,[12] C. Riedl,[10] K. Rith,[10] G. Rosner,[15] A. Rostomyan,[31] L. Rubacek,[14]
J. Rubin,[16] D. Ryckbosch,[13] Y. Salomatin,[23] I. Sanjiev,[2,22] I. Savin,[9] A. Schäfer,[24] C. Schill,[12] G. Schnell,[8]
K.P. Schüler,[7] J. Seele,[16] R. Seidl,[10] B. Seitz,[14] R. Shanidze,[10] C. Shearer,[15] T.-A. Shibata,[28] V. Shutov,[9]
M.C. Simani,[21,29] K. Sinram,[7] M. Stancari,[11] M. Statera,[11] E. Steffens,[10] J.J.M. Steijger,[21] H. Stenzel,[14] J. Stewart,[8]
F. Stinzing,[10] U. Stösslein,[6] P. Tait,[10] H. Tanaka,[28] S. Taroian,[31] B. Tchuiko,[23] A. Terkulov,[19] A. Tkabladze,[13]
A. Trzcinski,[30] M. Tytgat,[13] A. Vandenbroucke,[13] P. van der Nat,[21,29] G. van der Steenhoven,[21] M.C. Vetterli,[26,27]
V. Vikhrov,[22] M.G. Vincter,[1] C. Vogel,[10] M. Vogt,[10] J. Volmer,[8] C. Weiskopf,[10] J. Wendland,[26,27] J. Wilbert,[10]
G. Ybeles Smit,[29] Y. Ye,[5] Z. Ye,[5] S. Yen,[27] W. Yu,[4] B. Zihlmann,[21] H. Zohrabian,[31] and P. Zupranski[30]

(The HERMES Collaboration)

[1]*Department of Physics, University of Alberta, Edmonton, Alberta T6G 2J1, Canada*
[2]*Physics Division, Argonne National Laboratory, Argonne, Illinois 60439-4843, USA*
[3]*Istituto Nazionale di Fisica Nucleare, Sezione di Bari, 70124 Bari, Italy*
[4]*School of Physics, Peking University, Beijing 100871, China*
[5]*Department of Modern Physics, University of Science and Technology of China, Hefei, Anhui 230026, China*
[6]*Nuclear Physics Laboratory, University of Colorado, Boulder, Colorado 80309-0446, USA*
[7]*DESY, Deutsches Elektronen-Synchrotron, 22603 Hamburg, Germany*
[8]*DESY Zeuthen, 15738 Zeuthen, Germany*
[9]*Joint Institute for Nuclear Research, 141980 Dubna, Russia*
[10]*Physikalisches Institut, Universität Erlangen-Nürnberg, 91058 Erlangen, Germany*
[11]*Istituto Nazionale di Fisica Nucleare, Sezione di Ferrara and*
Dipartimento di Fisica, Università di Ferrara, 44100 Ferrara, Italy
[12]*Istituto Nazionale di Fisica Nucleare, Laboratori Nazionali di Frascati, 00044 Frascati, Italy*
[13]*Department of Subatomic and Radiation Physics, University of Gent, 9000 Gent, Belgium*
[14]*Physikalisches Institut, Universität Gießen, 35392 Gießen, Germany*
[15]*Department of Physics and Astronomy, University of Glasgow, Glasgow G12 8QQ, United Kingdom*
[16]*Department of Physics, University of Illinois, Urbana, Illinois 61801-3080, USA*
[17]*Laboratory for Nuclear Science, Massachusetts Institute of Technology, Cambridge, Massachusetts 02139, USA*
[18]*Randall Laboratory of Physics, University of Michigan, Ann Arbor, Michigan 48109-1120, USA*
[19]*Lebedev Physical Institute, 117924 Moscow, Russia*
[20]*Sektion Physik, Universität München, 85748 Garching, Germany*
[21]*Nationaal Instituut voor Kernfysica en Hoge-Energiefysica (NIKHEF), 1009 DB Amsterdam, The Netherlands*
[22]*Petersburg Nuclear Physics Institute, St. Petersburg, Gatchina, 188350 Russia*
[23]*Institute for High Energy Physics, Protvino, Moscow region, 142281 Russia*
[24]*Institut für Theoretische Physik, Universität Regensburg, 93040 Regensburg, Germany*
[25]*Istituto Nazionale di Fisica Nucleare, Sezione Roma 1, Gruppo Sanità*
and Physics Laboratory, Istituto Superiore di Sanità, 00161 Roma, Italy

[26]Department of Physics, Simon Fraser University, Burnaby, British Columbia V5A 1S6, Canada
[27]TRIUMF, Vancouver, British Columbia V6T 2A3, Canada
[28]Department of Physics, Tokyo Institute of Technology, Tokyo 152, Japan
[29]Department of Physics and Astronomy, Vrije Universiteit, 1081 HV Amsterdam, The Netherlands
[30]Andrzej Soltan Institute for Nuclear Studies, 00-689 Warsaw, Poland
[31]Yerevan Physics Institute, 375036 Yerevan, Armenia

Evidence for a narrow baryon state is found in quasi-real photoproduction on a deuterium target through the decay channel $pK_S^0 \to p\pi^+\pi^-$. A peak is observed in the pK_S^0 invariant mass spectrum at $1528 \pm 2.6(\text{stat}) \pm 2.1(\text{syst})$ MeV. Depending on the background model, the naïve statistical significance of the peak is 4–6 standard deviations and its width may be somewhat larger than the experimental resolution of $\sigma = 4.3$–6.2 MeV. This state may be interpreted as the predicted $S=+1$ exotic $\Theta^+(uudd\bar{s})$ pentaquark baryon. No signal for an hypothetical Θ^{++} baryon was observed in the pK^+ invariant mass distribution. The absence of such a signal indicates that an isotensor Θ is excluded and an isovector Θ is unlikely.

One of the central mysteries of hadronic physics has been the failure to observe baryon states beyond those whose quantum numbers can be explained in terms of three quark configurations. Exotic hadrons with manifestly more complex quark structures, in particular exotics consisting of five quarks, were proposed on the basis of quark and bag models [1] in the early days of QCD. The hope has been that the discovery of such objects would provide new insights into the dynamics of quark interactions in the strong coupling regime. Although it was hypothesized [2] that pentaquark systems involving heavy quarks, e.g. $uud\bar{c}s$, offered the most promising prospects for isolating such exotics, experimental searches carried out at FNAL [3] found no evidence for such states.

From quite a different point of view, it was noted [4, 5] that the Skyrme model predicts new exotic states belonging to higher SU(3) representations. Using this model, Praszalowicz [6] provided the first estimate of the mass of the lightest exotic state, $M \approx 1530$ MeV. Subsequently, an exotic baryon of spin 1/2, isospin 0, and strangeness $S=+1$ was discussed as a feature of the Chiral Quark Soliton model [5]. In this approach [7, 8] the baryons are rotational states of the soliton nucleon in spin and isospin space, and the lightest exotic baryon lies at the apex of an anti-decuplet with spin 1/2, which corresponds to the third rotational excitation in a three flavor system. Treating the known N(1710) resonance as a member of the anti-decuplet, Diakanov, Petrov, and Polyakov [8] derived a mass of 1530 MeV and a width of less than 15 MeV for this exotic baryon, since named the Θ^+. It corresponds to a $uudd\bar{s}$ configuration, and decays through the channels $\Theta^+ \to pK^0$ or nK^+. However, measurements of K^+ scattering on proton and deuteron targets showed no evidence [9] for strange baryon resonances, and appear to limit the width to remarkably small values of order an MeV. Presumably, the difficulty of experiments with kaon beams so close to threshold severely limited the

sensitivity to such narrow excitations. In a recent review of this subject [10], an experimental search by means of electro-production was suggested.

Experimental evidence for an exotic baryon first came recently [11] from the observation of a narrow resonance at $1540\pm10(\text{syst})$ MeV in the K^- missing mass spectrum for the $\gamma n \to K^+ K^- n$ reaction on ^{12}C. The decay mode corresponds to a $S=+1$ resonance and signals an exotic pentaquark state with quark content $(uudd\bar{s})$. Confirmation came quickly from a series of experiments, with the observation of sharp peaks [12–16] in the nK^+ and pK_S^0 invariant mass spectra near 1540 MeV, in each case with a width limited by the experimental resolution. The failure to observe a corresponding Θ^{++} peak in the pK^+ invariant mass spectrum in some of these experiments [13, 14] was taken to suggest that the state is an isospin singlet.

Alternative theoretical explanations have been proposed recently to explain this new exotic state. In one model, the Θ is described as an isotensor pentaquark [17], so that the narrow width results from the isospin-violating strong decay. A search for the decay of the isospin partners such as the $\Theta^{++}(uuud\bar{s})$ can provide a strong test of this idea. In a second interpretation, Karliner and Lipkin have developed a cluster model using a diquark-triquark configuration [18], in which the Θ^+ is also a positive-parity isosinglet member of an antidecuplet. Thirdly, using a model based on the strong color-spin correlation force, Jaffe and Wilczek [19] propose that the Θ^+ consists of two highly correlated ud pairs coupled to an $\bar{s}$. In their picture the positive-parity isosinglet Θ^+ lies at the apex of an nearly-ideally mixed SU(3)$_f$ $\mathbf{8_f} \oplus \overline{\mathbf{10_f}}$ multiplet. The narrowness of the 1530 MeV state is attributed to the relatively weak coupling of the kaon-nucleon continuum to the pentaquark $[ud]^2\bar{s}$ configuration.

The baryon states at the bottom two vertices of the anti-decuplet must also be manifestly exotic. Strong evidence in support of the baryon decuplet comes from the

reported observation of an exotic $S=-2$, $Q=-2$ baryon resonance in proton-proton collisions at $\sqrt{s} = 17.2\,\text{GeV}$ at the CERN SPS [20]. A narrow peak at a mass of about $1862\,\text{MeV}$ in the $\Xi^-\pi^-$ invariant mass spectrum is proposed as a candidate for the predicted exotic $\Xi^{--}_{\frac{3}{2}}$ baryon with $S=-2$, $I=\frac{3}{2}$ and a quark content of $(dsds\bar{u})$. At the same mass, a peak is observed that is a candidate for the $\Xi^0_{\frac{3}{2}}$ member of this isospin quartet. The corresponding anti-baryon spectra show enhancements at the same invariant mass. This observed mass of $1862\,\text{MeV}$ falls between the predictions of Refs. [8] and [19], although closer to the latter. Also, the positive parity for the Θ^+ predicted by these models contrasts with the negative parity suggested by the first lattice results [21, 22]. The general theoretical situation is still quite unsettled.

This Letter presents the results of a search for the Θ^+ in quasi-real photoproduction on deuterium. In addition to corroborating some features of the state measured previously, the data reported here provide more restrictive information related to its mass and isospin. The data were obtained by the HERMES experiment with the $27.6\,\text{GeV}$ positron beam of the HERA storage ring at DESY. Stored beam currents ranged from 9 to 45 mA. An integrated luminosity of $250\,\text{pb}^{-1}$ was collected on a longitudinally polarized deuterium gas target. The yields were summed over two spin orientations.

The HERMES spectrometer [23] consists of two identical halves located above and below the positron beam pipe, and has an angular acceptance of $\pm 170\,\text{mrad}$ horizontally, and $\pm(40 - 140)\,\text{mrad}$ vertically. The trigger was formed by either a coincidence between scintillating hodoscopes, a preshower detector and a lead-glass calorimeter, or a coincidence between three scintillating hodoscopes and two tracking planes, requiring that at least one charged track appears in each of the detector halves of the spectrometer.

The analysis searched for inclusive photoproduction of the Θ^+ followed by the decay $\Theta^+ \rightarrow pK^0_S \rightarrow p\pi^+\pi^-$. Events selected contained at least three tracks: two oppositely charged pions in coincidence with one proton. Identification of charged pions and protons was accomplished with a Ring-Imaging Čerenkov (RICH) detector [24] which provides separation of pions, kaons and protons over most of the kinematic acceptance of the spectrometer. The RICH identification efficiencies and cross contaminations had been determined in a limited kinematic domain using known particle species from identified resonance decays. However, because the RICH performance is sensitive to event topology, it was essential to determine these efficiencies and contaminations for pions and protons under conditions as close as possible to those of the present measurement. This was accomplished by means of a Monte Carlo simulation based on the PYTHIA6 generator discussed below. Events with the relevant topology were used to

determine these parameters as a function of particle momentum. The data from the simulation indicated that cross contaminations would be negligible if protons were restricted to a momentum range of 4–$9\,\text{GeV/c}$ and pions to a range of 1–$15\,\text{GeV/c}$, the kinematic restrictions subsequently used in the analysis.
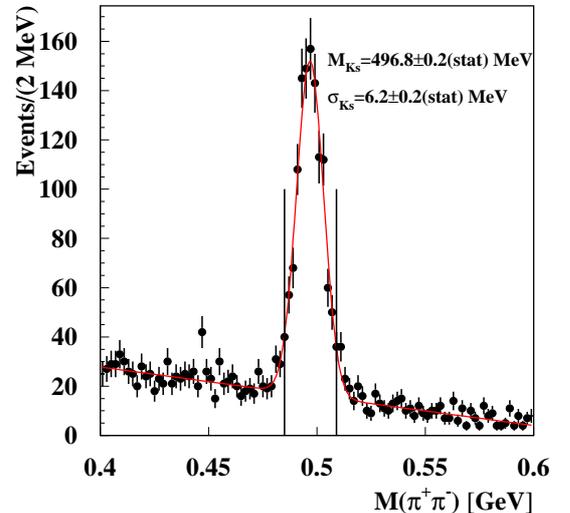

FIG. 1: Invariant mass distribution of two oppositely charged pions, subject to the constraints in event topology discussed in the text. A window corresponding to $\pm 2\,\sigma$ is shown by the vertical lines.

The event selection included constraints on the event topology to maximize the yield of the K^0_S peak in the $M_{\pi^+\pi^-}$ spectrum while minimizing its background. However, no constraints were optimized to increase the significance of the signal visible in the final $M_{p\pi^+\pi^-}$ spectrum, as such optimization would have produced a spectrum to which standard statistical tests do not apply. Based on the intrinsic tracking resolution, the required event topology included a minimum distance of approach between the two pion tracks less than $1\,\text{cm}$ (the midpoint of which is defined as the K^0_S decay vertex), a minimum distance of approach between the proton and reconstructed K^0_S tracks less than $6\,\text{mm}$ (the midpoint of which is defined as the production vertex), a radial distance of the production vertex from the positron beam axis less than $4\,\text{mm}$, a z coordinate of the production vertex within the $\pm 20\,\text{cm}$ long target cell of $-18\,\text{cm} < z < +18\,\text{cm}$ along the beam direction, and a K^0_S decay length (separation of production and K^0_S decay vertices) greater than $7\,\text{cm}$. To suppress contamination from the $\Lambda(1116)$ hyperon, events were rejected where the invariant mass $M_{p\pi^-}$ fell within $2\,\sigma$ of the nominal Λ mass, where $\sigma = 2.6\,\text{MeV}$ is the apparent width of the Λ peak observed in this experiment.

The resulting invariant $M_{\pi^+\pi^-}$ spectrum is shown in Fig. 1. The position of the K^0_S peak is within $1\,\text{MeV}$ of the expected value of $497.7 \pm 0.03\,\text{MeV}$ [25]. To

search for the Θ^+, events were selected with a $M_{\pi^+\pi^-}$ invariant mass within $\pm 2\,\sigma$ about the centroid of the K_S^0 peak. The resulting spectrum of the invariant mass of the $p\pi^+\pi^-$ system is displayed in Fig. 2. A narrow peak is observed. There is no known positively charged strangeness-containing baryon in this mass region (other than the Θ^+) that could account for the observed peak. Also, the $M_{p\pi^+\pi^-}$ spectrum corresponding to the sideband background adjacent to the K_S^0 peak in Fig. 1 was found to be featureless.
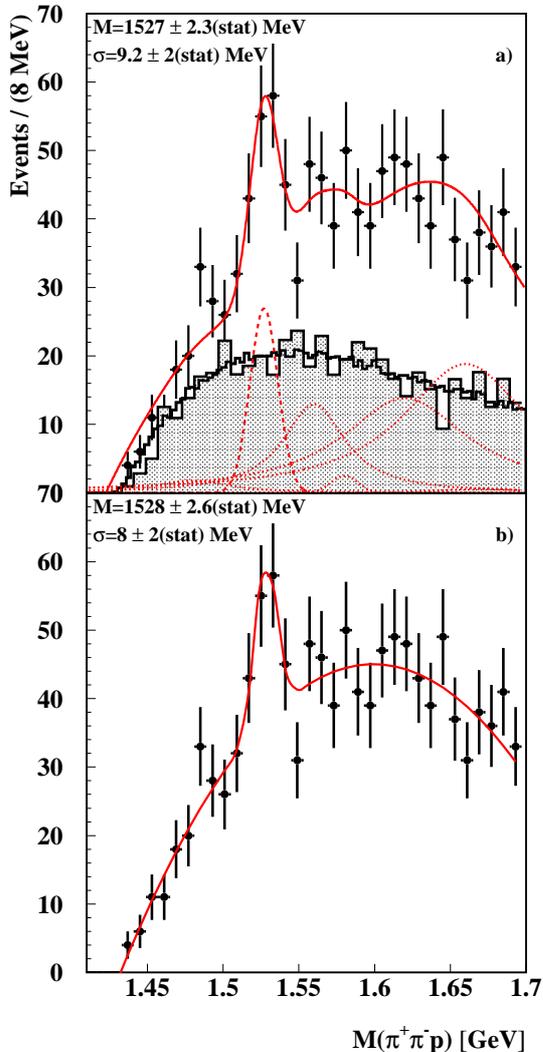

FIG. 2: Distribution in invariant mass of the $p\pi^+\pi^-$ system subject to various constraints described in the text. The experimental data are represented by the filled circles with statistical error bars, while the fitted smooth curves result in the indicated position and σ width of the peak of interest. In panel a), the PYTHIA6 Monte Carlo simulation is represented by the gray shaded histogram, the mixed-event model normalised to the PYTHIA6 simulation is represented by the fine-binned histogram, and the fitted curve is described in the text. In panel b), a fit to the data of a Gaussian plus a third-order polynomial is shown.

The non-resonant contribution to the spectrum was estimated by means of a simulation using a version of the PYTHIA6 code [26] tuned for HERMES kinematics [27]. This event generator contains no resonances in the mass range of Fig. 2a that decay in the pK_S^0 channel. The resulting simulated spectrum is shown in Fig. 2a as the gray hatched histogram. The statistical precision of the present study is limited by the rare topology of the events selected. Trigger inefficiencies were not included in the simulation, but are believed to be small. The simulated spectrum falls below the data at high invariant mass where Σ^{*+} resonances are known to exist [25]. Therefore, if PYTHIA6 is assumed to be capable of describing the shape of the non-resonant contribution, it can be concluded that there is substantial resonant strength distributed over the high-mass portion of the spectrum. At the position of the observed peak in the data, no corresponding structure appears in the simulated spectrum.

In order to determine the centroid, width and significance of the peak observed in Fig. 2, three different models for the background were explored. For the first model, the PYTHIA6 simulation is taken to represent the non-resonant background, and the remaining strength in the spectrum is attributed to a combination of known broad resonances and a new structure near 1.53 GeV. For the second model, it is assumed that the non-resonant background involves a large enough typical multiplicity that the 4-momenta of the K_S^0 and proton are largely uncorrelated. In this case, this background can be simulated by combining from different events a kaon and proton that satisfy the same kinematical requirements as the tracks taken from single events in the main analysis. Since resonances are typically visible only as rare correlations between their decay particles, their contributions will be relatively suppressed in this method. Fig. 2a shows that this procedure yields a shape that is very similar to that from the PYTHIA6 simulation, within the available statistics. By fitting a polynomial to the mixed-event background normalized to the PYTHIA6 simulation, and then fitting this polynomial together with the amplitudes of peaks for six known Σ^{*+} resonances in the mass range shown in Fig. 2 (dotted curves), plus all parameters of a narrow Gaussian (dashed curve) for the peak of interest, a good description of the entire spectrum is obtained. This procedure is intended to demonstrate that the background is consistent with known information. The included Σ^{*+} resonances were assigned fixed values of $M = 1480\,\mathrm{MeV}$ with $\Gamma = 55\,\mathrm{MeV}$ (PDG status = *), $M = 1560\,\mathrm{MeV}$ with $\Gamma = 47\,\mathrm{MeV}$ (**), $M = 1580\,\mathrm{MeV}$ with $\Gamma = 13\,\mathrm{MeV}$ (**), $M = 1620$ and $1660\,\mathrm{MeV}$ with $\Gamma = 100\,\mathrm{MeV}$ (***), and $M = 1670\,\mathrm{MeV}$ with $\Gamma = 60\,\mathrm{MeV}$ (****) [25]. Each intrinsic Breit-Wigner width was taken as the midpoint of the range of listed measurements, and was then augmented by an instrumental resolution of FWHM= 14.3 MeV added in quadrature. Since the $\Sigma^+(1580)$ has a width smaller than

TABLE I: Mass values and experimental widths, with their statistical and systematic uncertainties, for the Θ^+ from the two fits, labelled by a) and b), shown in the corresponding panels of Fig. 2. Rows a') and b') are based on the same background models as rows a) and b) respectively, but a different mass reconstruction expression that is expected to result in better resolution. Also shown are the number of events in the peak N_s and the background N_b, both evaluated from the functions fitted to the mass distribution, and the results for the naïve significance $N_s^{2\sigma}/\sqrt{N_b^{2\sigma}}$ and realistic significance $N_s/\delta N_s$. The systematic uncertainties are common (correlated) between rows of the table.

	Θ^+ mass [MeV]	FWHM [MeV]	$N_s^{2\sigma}$ in $\pm 2\sigma$	$N_b^{2\sigma}$ in $\pm 2\sigma$	naïve signif.	Total $N_s \pm \delta N_s$	signif.
a)	$1527.0 \pm 2.3 \pm 2.1$	$22 \pm 5 \pm 2$	74	145	$6.1\,\sigma$	78 ± 18	$4.3\,\sigma$
a')	$1527.0 \pm 2.5 \pm 2.1$	$24 \pm 5 \pm 2$	79	158	$6.3\,\sigma$	83 ± 20	$4.2\,\sigma$
b)	$1528.0 \pm 2.6 \pm 2.1$	$19 \pm 5 \pm 2$	56	144	$4.7\,\sigma$	59 ± 16	$3.7\,\sigma$
b')	$1527.8 \pm 3.0 \pm 2.1$	$20 \pm 5 \pm 2$	52	155	$4.2\,\sigma$	54 ± 16	$3.4\,\sigma$

the instrumental resolution, it was taken to be Gaussian with $\sigma = 8.9\,\mathrm{MeV}$. The numerical results of the fit are given in row a) of Table I. In addition, row a') shows the result of applying the same method to a mass spectrum based on an expression that is expected to provide an instrumental resolution improved by about 30%:

$$M'_{pK_S^0}{}^2 \equiv \left(\sqrt{M_p^2 + \mathbf{p}_p^2} + \sqrt{M_{K_S^0}^2 + \mathbf{p}_{K_S^0}^2}\right)^2 - (\mathbf{p}_p + \mathbf{p}_{K_S^0})^2, \tag{1}$$

where $M_{K_S^0}$ is taken from the PDG [25]. The third approach is based on the hypothesis that all of the background strength in the observed spectrum (apart from the narrow peak) can be described by a slowly varying function that extends under the feature of interest. Hence, the spectrum was fit with a Gaussian plus a polynomial. The appropriate degree of the polynomial used in the fit was determined by comparing results using orthonormal Chebyshev polynomials of various degrees. The curve shown in Fig. 2b results from a fit with a third-order polynomial, and rows b) and b') of Table I gives the numerical values from so fitting the two spectra corresponding to rows a) and a').

More specifically, Table I compares the results from the two fits for the centroid of the peak of interest, its width and the statistical significance according to two different prescriptions discussed below. The resulting values for the centroid are found to be consistent, while the width and significance depend on the method chosen to describe the remaining strength of the spectrum. Table I also lists for both fits the number of events given by the fitted function for the peak of interest ($N_s^{2\sigma}$) as well as for the background ($N_b^{2\sigma}$), in the invariant mass interval corresponding to $\pm 2\,\sigma$. The full area N_s of the Gaussian fitted to the peak of interest is also given with its uncertainty from the fit. This area itself, together with the width, were chosen to be explicit fit parameters to avoid the effect on the uncertainty in the area of correlations between the amplitude and the width or background parameters. All of these results are from unbinned maximum likelihood fits [28] to the original event

distributions, as it was found that the results of fitting the histograms shown in Fig. 2 can be sensitive to the choice of bin size or starting offset.

Several alternative expressions for the significance of the peak observed in Fig. 2 were considered. The first expression is the naïve estimator $N_s^{2\sigma}/\sqrt{N_b^{2\sigma}}$ used in Refs. [11–16]. The corresponding result is listed in Table I. Because this statistic neglects the uncertainty in the background fit, it overestimates the significance of the peak [29]. A second estimator that was used in the analysis presented in Ref. [20], $N_s^{2\sigma}/\sqrt{N_s^{2\sigma} + N_b^{2\sigma}}$, gives a somewhat lower value, but may still underestimate the background uncertainty. A third estimate of the significance is given by $N_s/\delta N_s$, where N_s is now the full area of the peak from the fit and δN_s is its fully correlated uncertainty. This ratio measures how far the peak is away from zero in units of its own standard deviation. All correlated uncertainties from the fit, including those of the background parameters, are accounted for in δN_s. The results obtained with this expression are also given in Table I.

The systematic uncertainty of the mass of the state observed in Fig. 2 is estimated to be $\pm 2.1\,\mathrm{MeV}$ by adding in quadrature a contribution of $1\,\mathrm{MeV}$ to account for the effect of using different spectrum analysis methods (cf. Table I) plus a contribution of $1.9\,\mathrm{MeV}$ from the precision with which the spectrometer can reproduce known particle masses (cf. Table II). The $1.9\,\mathrm{MeV}$ contribution to the systematic uncertainty accounts for both the discrepancies from the PDG [25] mass values and the statistical precision of their fits. As an example, the $\Lambda(1520)$ mass peak fitted with a Gaussian with free width convoluted with a Breit-Wigner form with its width fixed at the PDG value [25] is shown in the M_{pK^-} spectrum of Fig. 3. The event selection for the spectra in this figure is the same as for the pK_S^0 analysis, except the reconstructed K_S^0 track is replaced by that of the observed charged kaon, which is required to have a minimum momentum of $3\,\mathrm{GeV}$.

The mass values reported to date for the Θ^+ state by other experiments are compared to the present results in

TABLE II: Masses and widths of observed invariant mass peaks for four known particles, compared to the known masses [25] and the widths obtained from a Monte Carlo simulation of the spectrometer. (The widths for the $\Xi^-(1321)$ are from mass-difference spectra.) The $\Lambda(1520)$ peak of Fig. 3 was fitted with a Gaussian folded with a Breit-Wigner form whose Γ width was fixed at the PDG value (15.6 MeV). The uncertainties in the resulting mass and Gaussian σ width were inflated by the factor $\sqrt{\chi^2/N_{dof}}$. In the last row, P_{cm} is the momentum of each decay product in the rest frame of the decaying particle.

	$K_S^0 \to \pi^+\pi^-$	$\Lambda(1116) \to p\pi^-$	$\Lambda(1520) \to pK^-$	$\Xi^-(1321) \to p\pi^-\pi^-$
Observed mass [MeV]	496.8 ± 0.2	1115.70 ± 0.01	1522.7 ± 1.9	1321.5 ± 0.3
PDG Mass [MeV]	497.67	1115.68	1519.5 ± 1.0	1321.31 ± 0.13
σ Width (data) [MeV]	6.2 ± 0.2	2.6 ± 0.1	4.4 ± 3.7	3.1 ± 0.3
σ Width (MC) [MeV]	5.4	2.1	3.5	2.5
Decay P_{cm} [MeV/c]	206	101	244	139 ($\Lambda\pi^-$)

Fig. 4, and listed in Table III . The systematic uncertainties of the DIANA and ITEP measurements were taken to be ± 3 MeV in the absence of explicit values quoted in the corresponding papers [12, 15]. By fitting the data with a constant, a reduced χ^2 value of $12.41/6$ is found, corresponding to a confidence level of 0.053 as defined in the PDG [25]. The weighted average [25] of the masses observed in all experiments is 1536.2 ± 2.6 MeV, which is represented by the shaded band in Fig. 4. In evaluating this average mass value, the quadratic sum of the statistical and systematic uncertainties of all measurements are taken into account. The uncertainty of the average was scaled by the usual factor of square root of the reduced χ^2.

Since no realistic model for the photoproduction of exotic baryons at this experiment's energy is presently available, a "toy Monte Carlo" was produced to study the constraints imposed on the decay products by only

kinematics and acceptance. It generates parent particles with specified mass and width, at vertices distributed according to the HERMES target gas profile. The generated events were then passed to a full simulation of the spectrometer that included the performance of the RICH. The unknown kinematic distribution of the parent in transverse momentum P_t was taken to be Gaussian with a width of $\sigma = 0.4$ GeV, which is typical of intrinsic transverse momentum of partons or transverse momentum induced by the fragmentation process, and also corresponds to the root-mean-square value of the transverse momentum distribution of $\Lambda(1116)$ and $\bar{\Lambda}$ hyperons that are observed at HERMES. The simulated acceptance was found to be fairly insensitive to this parameter. The lon-
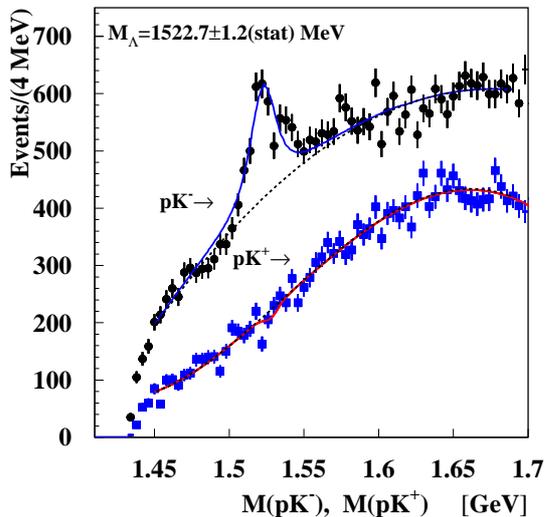

FIG. 3: Spectra of invariant mass M_{pK^-} (top) and M_{pK^+} (bottom). A clear peak is seen for the $\Lambda(1520)$ in the M_{pK^-} invariant mass distribution. However, no peak structure is seen for the hypothetical Θ^{++} in the M_{pK^+} invariant mass distribution near 1.53 GeV.
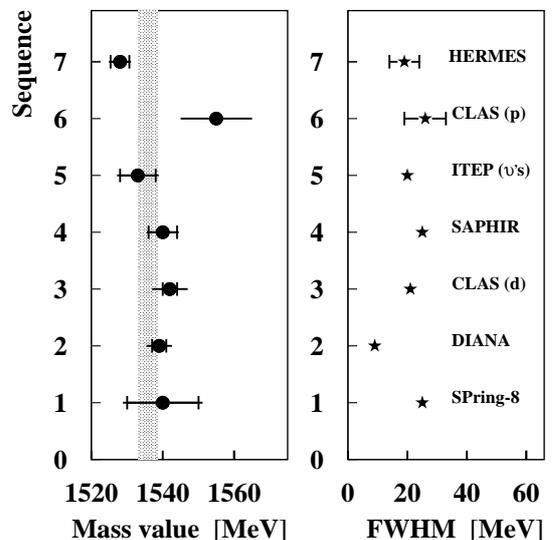

FIG. 4: Mass values and experimental FWHM widths observed in various experiments for the Θ^+ state. The inner error bars represent the statistical uncertainties, and the outer error bars represent the quadratic sum of the statistical and systematic uncertainties. (Some uncertainties for the widths are not available from the other experiments.) The hatched area corresponds to the weighted average of all data ± 1 standard deviation.

TABLE III: Mass values and experimental widths for the Θ^+ state as observed in the various experiments. The present result is also listed. In calculating the weighted average of the data, the systematic uncertainties of DIANA and ITEP are taken to be ± 3 MeV.

Experiment	Θ^+ mass (MeV)	FWHM (MeV)	Ref.
SPring8	$1540 \pm 10 \pm 5$	25	[11]
DIANA	$1539 \pm 2 \pm$ "few"	9	[12]
CLAS (d)	$1542 \pm 2 \pm 5$	21	[13]
SAPHIR	$1540 \pm 4 \pm 2$	25	[14]
ITEP (ν's)	1533 ± 5	20	[15]
CLAS (p)	$1555 \pm 1 \pm 10$	26 ± 7	[16]
HERMES	$1528 \pm 2.6 \pm 2.1$	$19 \pm 5 \pm 2$	
world average	1536.2 ± 2.6		

gitudinal momentum P_z was assigned a monotonically falling distribution similar to what has been observed for Λ hyperons at HERMES. The acceptance for the $pK^\pm$ final state is insensitive to this choice, but this is not the case for the $p\pi^+\pi^-$ final state, where drastically different assumptions can result in a factor of two change in the acceptance. The full width Γ of the Θ^+ was chosen to be 2 MeV, according to the limit recently derived from a review of KN phase shift analyses [9]. The effect of such an intrinsic width is small compared to that of the spectrometer resolution, which was found in this simulation to be $\sigma = 6.2$ MeV in $M_{p\pi^+\pi^-}$, or 4.3 MeV in $M'_{pK^0_S}$ of Eq. 1. These values are assigned a systematic uncertainty of ± 1 MeV, based on the level of agreement between observed and simulated widths of four known particles, as shown in Table II.

The width of the peak of interest in Fig. 2, given in Table I, is somewhat larger than the instrumental resolution derived from the simulation. An attempt was made to repeat the fits of Table I using for the peak of interest a Breit-Wigner form convoluted with a Gaussian whose width was fixed at the simulated resolution.[1] The resulting mass values are consistent with those given in Table I, and the resulting values for the intrinsic width are $\Gamma = 12 \pm 9(\text{stat}) \pm 3(\text{syst})$ MeV in case a) of Table I, $\Gamma = 20 \pm 8(\text{stat}) \pm 3(\text{syst})$ MeV in case a'), $\Gamma = 8 \pm 8(\text{stat}) \pm 3(\text{syst})$ MeV in case b), and $\Gamma = 13 \pm 9(\text{stat}) \pm 3(\text{syst})$ MeV in case b'). The systematic uncertainties here correspond only to the $\delta\sigma = \pm 1$ MeV uncertainty in the instrumental resolution, which was discussed above.

In view of the speculation that the observed resonance is isotensor [17], the possibility that the Θ^{++} partner is

---

[1] The software tool RooVoigtian was used, for unbinned fitting.

present in the M_{pK^+} spectrum was explored. Although Fig. 3 shows a clear peak for the $\Lambda(1520)$ in the M_{pK^-} invariant mass spectrum, there is no peak structure observed in the M_{pK^+} invariant mass distribution. From a fit (curve in Fig. 3) of the M_{pK^+} distribution using a free polynomial plus a Gaussian with the fixed location (± 5 MeV) from the fit in Fig. 2b and a fixed width corresponding to the simulated peak width of $\sigma = 4.5$ MeV in this decay channel, the Gaussian area for a hypothetical Θ^{++} peak is found to be -40 ± 30 events. This result is robust against varying the order of the polynomial background. It corresponds to an upper limit of zero counts at the 91% confidence level.

The failure to observe a Θ^{++} suggests that the Θ is likely to be isoscalar. However, in the situation more probable at lower beam energy that the Θ is produced only via the exclusive reaction $\gamma + p \to \Theta + K$ without any other hadrons in the final state, the following limitations would apply to deductions about its isospin. Under the assumption of isospin symmetry, selection rules limit the transition amplitude for forming a tensor Θ to a single reduced matrix element for an isovector transition. In this case, production of the Θ^{++} and the Θ^+ are expected to have comparable strength, and the failure to observe the Θ^{++} rules out the $I = 2$ assignment. Production of an isovector Θ would arise from a sum of three reduced amplitudes with unknown magnitudes and phases. With only model-dependent values for these amplitudes, no precise statement can be made about the relative yields of the Θ^{++} and Θ^+. However, because a nearly complete cancellation is improbable, the failure to observe the Θ^{++} indicates that an isovector Θ is unlikely.

Estimates of the spectrometer acceptance times efficiency from the toy Monte Carlo simulation can be used to estimate some cross sections. Using the assumptions about the initial kinematic distribution described above and assuming that the decay angle distribution is flat, these acceptances were estimated to be 1.5% for both $\Lambda(1520) \to pK^-$ and $\Theta^{++} \to pK^+$, and 0.05% for $\Theta^+ \to pK^0_S$. Taking the branching fraction of the Θ^+ to pK^0_S to be $(1/2) \cdot (1/2)$ (to account for competition with both the nK^+ channel and K^0_L), the cross section for its photoproduction is found to range from about 100 to 220 nb $\pm 25\%(\text{stat})$, depending on the model for the background and the functional form fitted to the peak. The cross section for photoproduction of the $\Lambda(1520)$ is found to be $62 \pm 11(\text{stat})$ nb. Hence the ratio of the Θ^+ cross section to that for the $\Lambda(1520)$ is found to lie between 1.6 and 3.5. All of these estimates are subject to an additional factor of two uncertainty, to account for the assumptions about the kinematic distribution of the parents used in the simulation as explained above, and neglected trigger inefficiencies.

In conclusion, evidence has been obtained in quasi-real photoproduction on a deuterium target for a narrow baryon state in the pK^0_S invariant mass spectrum

at $1528 \pm 2.6(\text{stat}) \pm 2.1(\text{syst})\,\text{MeV}$. Depending on the background model, the width of the observed peak may be larger than the experimental resolution of $\sigma =4.3$–$6.2\,\text{MeV}$. Fitting the peak with a convolution of a Breit-Wigner shape with a Gaussian representing the simulated instrumental resolution yields an extracted intrinsic width $\Gamma = 17 \pm 9(\text{stat})\pm3(\text{syst})\,\text{MeV}$ (the average of the results from cases a' and b' of Table I). The significance of the observed state expressed as $N_s^{2\sigma}/\sqrt{N_b^{2\sigma}}$ ranges from $4.2\,\sigma$ to $6.3\,\sigma$, and expressed as $N_s/\delta N_s$ ranges from $3.4\,\sigma$ to $4.3\,\sigma$, again depending on the model for the background. This observation provides further evidence for the existence of a narrow baryon state with $|S| = 1$ and a mass in the region where such a feature was observed by earlier experiments. Formally, the difference between the value for the mass derived here and that from the other experiments reduces the confidence level of the combined fit to all mass data from 0.57 to 0.053, a value still typical for well-established particles [25]. There is no identified Σ^{*+} state with $S=-1$ in the invariant mass region between 1500 and $1550\,\text{MeV}$. Therefore, the state observed here may be interpreted as the predicted exotic Θ^+ pentaquark $S=+1$ baryon. The absence of a corresponding signal in the pK^+ invariant mass spectrum indicates that the observed Θ^+ is not isotensor and is probably an isosinglet.

[1] R.L. Jaffe, Proc. Topical Conference on Baryon Resonances, Oxford, July 1976, SLAC-PUB-1774.

[2] H.J. Lipkin, Phys. Lett. B **195**, 484 (1987); C. Gignoux, B. SilvestreBrac, and J.M. Richard, Phys. Lett. B **193**, 323 (1987).

[3] M.A. Moinester *et al.*, Z. Phys. A **356**, 207 (1996).

[4] A. Manohar, Nucl. Phys. B **248**, 19 (1984).

[5] M. Chemtob, Nucl. Phys. B **256**, 600 (1985).

[6] M. Praszalowicz, "Workshop on Skyrmions and Anomalies", M. Jezabek and M. Praszalowicz editors, World Scientific, 1987, page 112; M. Praszalowicz, Phys. Lett. B **575**, 234 (2003).

[7] H. Walliser, Nucl. Phys. A **548**, 649 (1992).

[8] D. Diakonov, V. Petrov, and M. Polyakov, Z. Phys. A **359**, 305 (1997).

[9] R. Arndt, I. Strakovsky, and R. Workman, Phys. Rev. C **68**, 042201 (2003); nucl-th/0311030.

[10] H. Gao and B.-Q. Ma, Mod. Phys. Lett. A **14**, 2313 (1999).

[11] T. Nakano *et al.*, Phys. Rev. Lett. **91**, 012002 (2003).

[12] DIANA Collaboration, V.V. Barmin *et al.*, Phys. Atom. Nucl. **66**, 1715 (2003); Yad. Fiz. **66**, 1763 (2003).

[13] CLAS Collaboration, S. Stepanyan *et al.*, hep-ex/0307018, and K. Hicks, private communications.

[14] SAPHIR Collaboration, J. Barth *et al.*, Phys. Lett. B **572**, 127 (2003).

[15] A. E. Asratyan *et al.*, hep-ex/0309042.

[16] CLAS Collaboration, V. Kubarovsky *et al.*, hep-ex/0311046.

[17] S. Capstick *et al.*, Phys. Lett. B **570**, 185 (2003).

[18] M. Karliner and H.J. Lipkin, Phys. Lett. B **575**, 249 (2003).

[19] R. Jaffe and F. Wilczek, Phys. Rev. Lett. **91**, 232003 (2003).

[20] NA49 Collaboration, C. Alt *et al.*, hep-ex/0310014.

[21] S. Sasaki, hep-lat/0310014.

[22] F. Csikor, Z. Fodor, S. D. Katz and T. G. Kovacs, hep-lat/0309090.

[23] HERMES Collaboration, K. Ackerstaff *et al.*, Nucl. Instr. Meth. A **417**, 230 (1998).

[24] N. Akopov *et al.*, Nucl. Instr. Meth. A **479**, 511 (2002).

[25] Particle Data Group, K. Hagiwara *et al.*, Phys. Rev. D **66**, 010001 (2002).

[26] T. Sjöstrand *et al.*, Comput. Phys. Commun. **135**, 238 (2001).

[27] E.-C. Aschenauer, P. Liebing, and T. Sjöstrand, in preparation.

[28] W. Verkerke and D. Kirkby, "The Roofit toolkit for data Modeling", physics/0306116.

[29] W.T. Eadie *et al.*, "Statistical Methods in Experimental Physics", North-Holland Publishing Company, p. 273, Eq. 11.20.